JOURNAL OF MATERIALS SCIENCE 22 (1987) 76–84

Relation of transformation temperature to the fracture toughness of transformation-toughened ceramics

PAUL F. BECHER
Metals and Ceramics Division, Oak Ridge National Laboratory, Oak Ridge, Tennessee 37831, USA

M. V. SWAIN
Advanced Materials Laboratory, CSIRO, Melbourne, Victoria 3168, Australia

M. K. FERBER
Ceramic Engineering Department, University of Illinois, Champaign-Urbana, Illinois 61801, USA

The stress induced tetragonal to monoclinic ZrO_2 martensitic transformation contribution to fracture toughness is described in terms of the required external strain energy and the thermodynamic stability of the constrained tetragonal phase. The strain energy, derived from an externally applied stress acting on the main crack, required to achieve transformation toughening is shown to be a function of the term $(T - M_s)$ where T is the test temperature and M_s is the martensite start temperature for the case of $T > M_s$. Thus for a given T $(T > M_s)$, the transformation toughening component increases as M_s approaches T and for a fixed M_s, the toughness decreases as T increases. Experimental data for partially stabilized zirconia ceramics confirm these results and show that increasing tetragonal precipitate size is the primary feature which affects an increase in M_s. In the case of $T \leqslant M_s$, autotransformation occurs, resulting in decreasing toughness with decrease in T due to a continuous loss in the tetragonal phase content. A temperature region is thus obtained over which transformation toughening exhibits a maximum in its contribution. The temperatures over which this occurs then is shown to be dependent on the M_s temperature of the material.

1. Introduction

In the case of ZrO_2, the tetragonal to monoclinic transformation involves a volume increase as well as a shear strain. Thus under conditions where the sample is stressed, the transformation occurs in a tensile strain field (e.g. that surrounding a crack tip) which allows the volume to expand. Observations reveal that the shear (shape change) strain is often minimized by the generation of twins within the monoclinic phase [1, 2]. When they transform and expand, the ZrO_2 particles introduce radial compressive strains in the surrounding matrix. As the volume increase is 5 to 6% [3, 4] the linear compressive strains in the matrix are quite large (1 to 2%). In this case the associated local compressive stresses are very high (0.01 to 0.02 times the Young's modulus of the matrix) and modify (decrease) any nearby tensile stress fields. Thus the externally applied tensile stress must be increased to raise the local tensile stress field to its former level near a transformed particle. When tetragonal ZrO_2 particles transform in the tensile stress field of a crack tip, the crack tip tensile stress is decreased and the external tensile stress must be increased to generate sufficient tensile stress to continue to propagate the crack. This is clearly why this type of transformation is so attractive in ceramics, where cracks normally grow quite easily when subjected to very modest tensile stress conditions.

The tetragonal to monoclinic phase transformation in ZrO_2 can be characterized by the temperatures at which the forward (M_s) and reverse (A_s) transformations are initiated during decreasing and increasing temperature cycles, respectively. At $T = M_s$, a portion of the constrained tetragonal precipitates/particles spontaneously transforms to the monoclinic phase so that the total energy change, ΔG_T^{t-m}, must be zero [5], the total energy change being the sum of the changes in chemical free, surface, and internal strain energies. When $T > M_s$, $\Delta G_T^{t-m} > 0$ and additional energy must be supplied to initiate the transformation. This can be derived from the strain energy introduced from an externally applied tensile stress. When ΔG_T^{t-m} is still positive but is decreased towards zero, the amount of externally supplied strain energy, ΔU_{se}, required is likewise decreased.

In the case of transformation-toughened materials, determination of the M_s temperatures for different compositions and microstructures (e.g. precipitate size) should be useful in describing the stability of the tetragonal phase and hence should provide an indication of the toughness of each material. Again when

0022–2461/87 $03.00 + .12

$T = M_s$, $\Delta G_T^{\text{t-m}}$ is zero and the transformation is initiated spontaneously as seen by

$$\Delta G_T^{\text{t-m}} = (T - M_s)\Delta S \qquad (1)$$

where T represents the temperature of interest and ΔS is the entropy difference between the two phases [5]. Thus when $T > M_s$ the tetragonal phase is stable, and some external energy must be supplied to transform it. This is, of course, the case of interest in transformation-toughened systems where the strain energy supplied by an external tensile stress triggers the transformation.

The critical stress (σ_c^T) required to transform a tetragonal precipitate/particle is related to the external applied strain energy required ($\Delta U_{\text{se}} = \Delta G_T^{\text{t-m}}$) to initiate the transformation:

$$\Delta U_{\text{se}} = \sigma_c^T e^T \qquad (2)$$

so that

$$\sigma_c^T = \Delta G_T^{\text{t-m}}/e^T \qquad (3)$$

where e^T is the volume expansion strain.

The incremental increase in the fracture toughness due to the transformation (ΔK_{IC}^T) is related to the half-width of the transformed zone surrounding the crack (r) by

$$\Delta K_{\text{IC}}^T = A e^T V_f E^c r^{1/2} \qquad (4)$$

where A is a function of the form of the transformation stress ($A = 0.22$ for transformations triggered by the principal stress and $A = 0.50$ for those initiated by shear stress [6]), V_f is the volume fraction of transformable ZrO_2, and E^c is Young's modulus of the system. Analogous to the plastic zone size in metals, the transformation zone size is a function of the critical transformation stress:

$$r = B(K_{\text{IC}}^{\text{M}}/\sigma_c^T)^2 \qquad (5)$$

where K_{IC}^{M} is the fracture toughness of the matrix. The term B is equal to $[2(1 + \nu)^2/9\pi]$ where ν is Poisson's ratio and the term accounts for the geometry of the crack tip stress field [7]. By combining Equations 3, 4 and 5, we find that

$$\Delta K_{\text{IC}}^T = AB^{1/2}(e^T)^2 V_f E^c K_{\text{IC}}^{\text{M}}/(\Delta G_T^{\text{t-m}}) \qquad (6)$$

and by substitution of Equation 3, we obtain

$$\Delta K_{\text{IC}}^T = AB^{1/2}(e^T)^2 V_f E^c K_{\text{IC}}^{\text{M}}/\Delta S(T - M_s) \qquad (7)$$

and the dependence of the toughness on the test temperature and the transformation temperature of the material.

As one expects, the above relationship predicts that the fracture toughness due to the transformation decreases as the reciprocal of the increase in the test temperature for each material for a fixed value of M_s. This is consistent with the increase in stability of the transforming tetragonal phase with increase in test temperature, and also predicts that the critical transformation stress increases (Equations 1 and 3) and the zone size decreases (Equation 5) as either the test temperature increases or M_s decreases. A similar increase in toughness is predicted as M_s approaches T for the case of $T > M_s$. Thus, a maximum in toughness can be achieved by increasing the M_s temperature of ZrO_2 until it is nearly equal to the temperature of interest. Likewise, the toughness of a given ZrO_2 will reach a maximum as the test temperature is lowered to its M_s temperature. In order to test these relationships, a series of MgO–PSZ ceramics were systematically examined and characterized in terms of toughness, transformation temperatures, and microstructure/composition.

2. Experimental procedures

Several partially stabilized zirconia (PSZ) ceramics which contained MgO were characterized as to critical fracture toughness including the effect of test temperature, transformation temperatures, microstructures, phase content and composition. The critical fracture toughness, K_{IC}, values were obtained with either the applied-moment double cantilever method [8] or the technique based upon fracture of polished flexure bars containing multiple indent cracks [9]. In many cases, both methods were used (except at elevated temperatures) in order to verify the results obtained by these techniques. The agreement between these two techniques was very good, with the mean values of each within one standard deviation of the other. At elevated temperatures, the fracture of polished flexure bars containing indent cracks in their tensile surfaces was used exclusively to obtain K_{IC} values.

The transformation temperatures were derived from the thermal expansion hysteresis generated by the tetragonal to monoclinic transformation during cooling of the samples and the reverse transformation during heating. The expansion data were obtained using a dual-rod dilatomer (Theta, Port Washington, New York) with a furnace capable of heating the samples from room temperature to 1600° C. A liquid-nitrogen cooled chamber was fabricated which allowed the samples to be cooled from room temperature to at least −190° C in a flowing helium gas environment which was first passed through a liquid nitrogen heat exchanger. For samples having M_s temperatures less than room temperature, it was necessary to first run the low temperature portion of the expansion and transform the tetragonal to the monoclinic phase. Only when this was accomplished could the elevated-temperature expansion hysteresis be accurately determined, as then the monoclinic phase can transform back to the tetragonal phase upon heating.

Finally, the microstructures of the PSZ ceramics were evaluated by scanning electron microscopy methods using polished samples which had been etched in 10% hydrofluoric acid for 2 to 5 min. The phase contents were then derived for ground surfaces, polished surfaces and polished surfaces after they had been air annealed at 1100° C for 0.5 h using X-ray diffraction with a copper target [10] and laser Raman spectroscopy data [11, 12]. Subsequently, the MgO and HfO_2 contents of the samples were obtained from data generated by electron microprobe analyses (Model 733, Jeol, Boston, Massachusetts) using multiple step scans, a 30 μm probe size and incorporated standards.

3. Observations and discussion

The thermal expansion hysteresis characteristics of

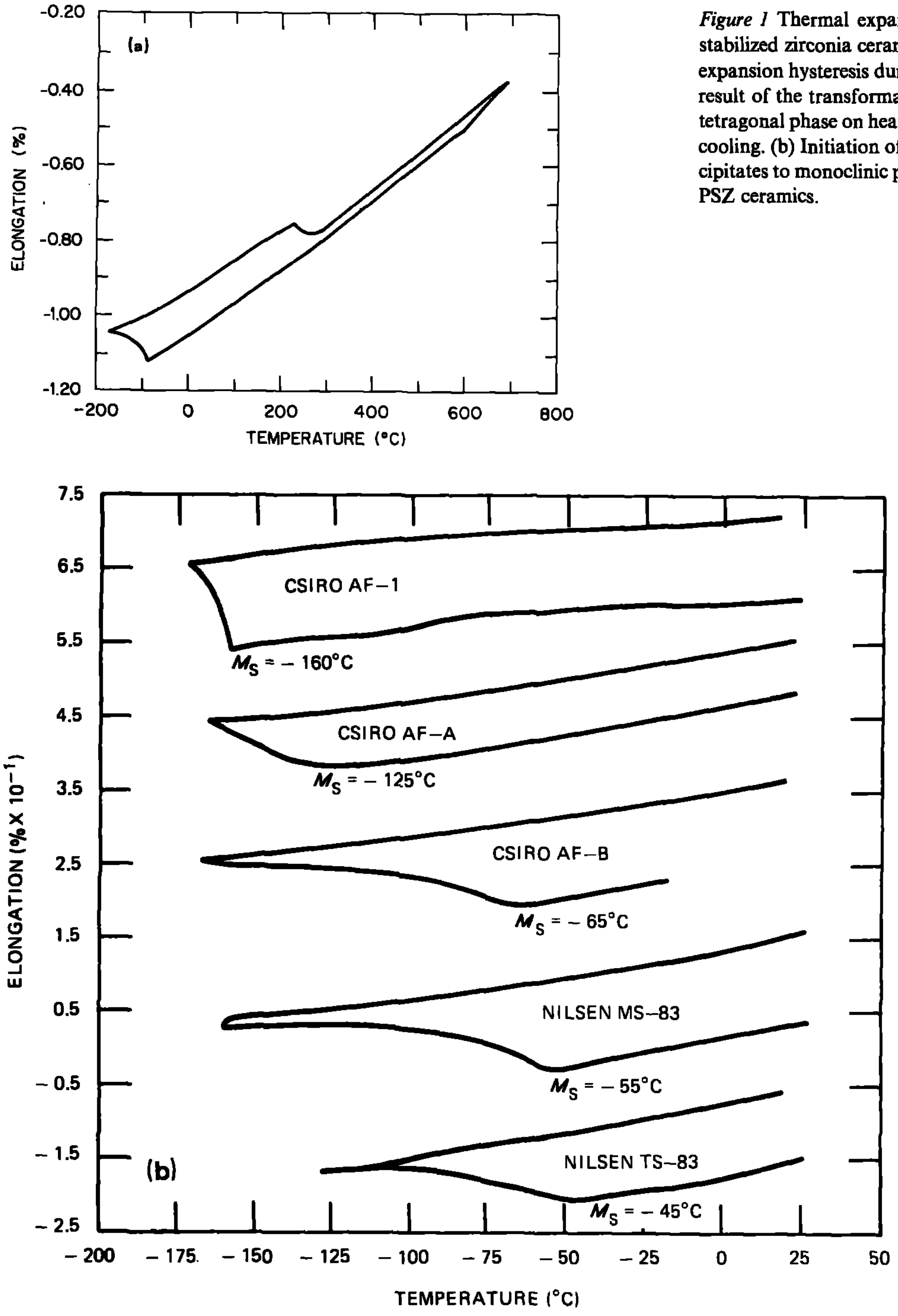

Figure 1 Thermal expansion curves for various partially stabilized zirconia ceramics containing MgO. (a) Thermal expansion hysteresis during heating and cooling cycles is a result of the transformation of monoclinic precipitates to tetragonal phase on heating and reverse transformation on cooling. (b) Initiation of transformation of tetragonal precipitates to monoclinic phase at M_s temperature for several PSZ ceramics.

several of the PSZ ceramics are illustrated in Fig. 1. Note that M_s and M_f denote the temperatures during cooling at which the tetragonal to monoclinic transformation is initiated and completed, respectively. A_s and A_f denote the temperatures at which the reverse transformation is initiated and completed during the heating cycle. The transformation temperatures for each material are listed in Table I; however, for samples exhibiting $M_s < 22°$ C the samples could not be cooled sufficiently to reach a true M_f temperature. Note that the TS grade PSZ ceramic labelled TS-83 exhibits two M_s temperatures which reflect two different tetragonal precipitate groups (discussed later).

One should keep in mind that in the MgO–PSZ system, the materials consist of tetragonal/monoclinic precipitates, a cubic matrix which in the present study had a grain size of about 60 μm, and often has eutectoid decomposition phases of monoclinic ZrO_2 and MgO at the matrix grain boundaries [13, 14]. This eutectoid decomposition can generate considerable monoclinic phase as a result of ageing the PSZ at temperatures even as low as 1000° C. As a result of this, not only is an elevated temperature M_s introduced, but the expansion hysteresis strain will increase as more monoclinic phase is generated by continued eutectoid decomposition.

The CSIRO samples consist of three as-fired samples of differing precipitate sizes, four samples that were subsequently aged at 1100° C for various times, and one sample aged at 1400° C for 8 h after firing. Representative microstructures of these samples are shown in Fig. 2. As can be seen, the precipitate sizes and the amount of grain-boundary euctectoid phases vary in these samples. As a result of these treatments,

TABLE I Typical characteristics of partially stabilized zirconia samples

Property	Sample designation				
	TS-82[‡]	TS-83[‡]	MS-83[‡]	AF-1[§]	Ag-1[§]
Transformation temperatures (° C)					
M_s	390	−45	−55	−160	260
M_f	80	< −185/20	< −155	< −175	20
A_s	520	205/390	230	200	545
A_f	825	300/670	285	255	710
Precipitate length (μm)/thickness (μm)					
	0.4/0.7	0.25/0.03	0.25/0.03	⩽0.20/0.02	0.45/0.08
	0.3/0.05	0.4/0.07	0.16/0.02		
Phase content					
%monoclinic[*]	44	14	6	1 to 3	38
tetragonal[†]	0	≳30	~37	5	⩽5
Composition (mol %)					
MgO	8.4	8.5	8.3	7.1	7.4
H_fO_2	0.9	0.9	0.9	1.3	1.2
K_{IC} at 22° C (MPa m$^{1/2}$)	6.2	12.5	14	8.5	6.3

[*] X-ray diffraction data, copper target, % monoclinic = $100\,[I_{m(111)}/(I_{m(111)} + I_{t+c(111)})]$.

[†] Values for % tetragonal phase in the cubic, monoclinic plus tetragonal mixture were obtained from laser Raman data where % tetragonal = $100\,[I_t/(I_t + I_m)]$ and X-ray data for the actual monoclinic content.

[‡] Nilsen Ceramics, Inc. (now Nilcra Ceramics USA), St. Charles, Illinois.

[§] Samples fabricated at CSIRO, Melbourne, Australia.

the percentage of monoclinic with respect to cubic and tetragonal phases (from the X-ray data) and the tetragonal to monoclinic ratio (from the laser Raman data) differ in each PSZ (Table I). The MS and TS grades of the Nilsen PSZ ceramics exhibit similar differences in both microstructure and phase contents (Table I and Fig. 2). In addition, the CSIRO PSZ ceramics contain less MgO than do the Nilsen PSZ ceramics (7.3 mol % compared with 8.4 mol %), (Table I). The variations in HfO_2 content at the low levels detected in these PSZ ceramics do not influence the transformation temperatures.

The observed relationship between the M_s temperatures and the precipitate sizes, shown in Fig. 3, indicates that M_s increases with increase in precipitate size. This is consistent with an increase in stress intensity acting on the precipitate which scales with particle size, due to the stress concentrating effects

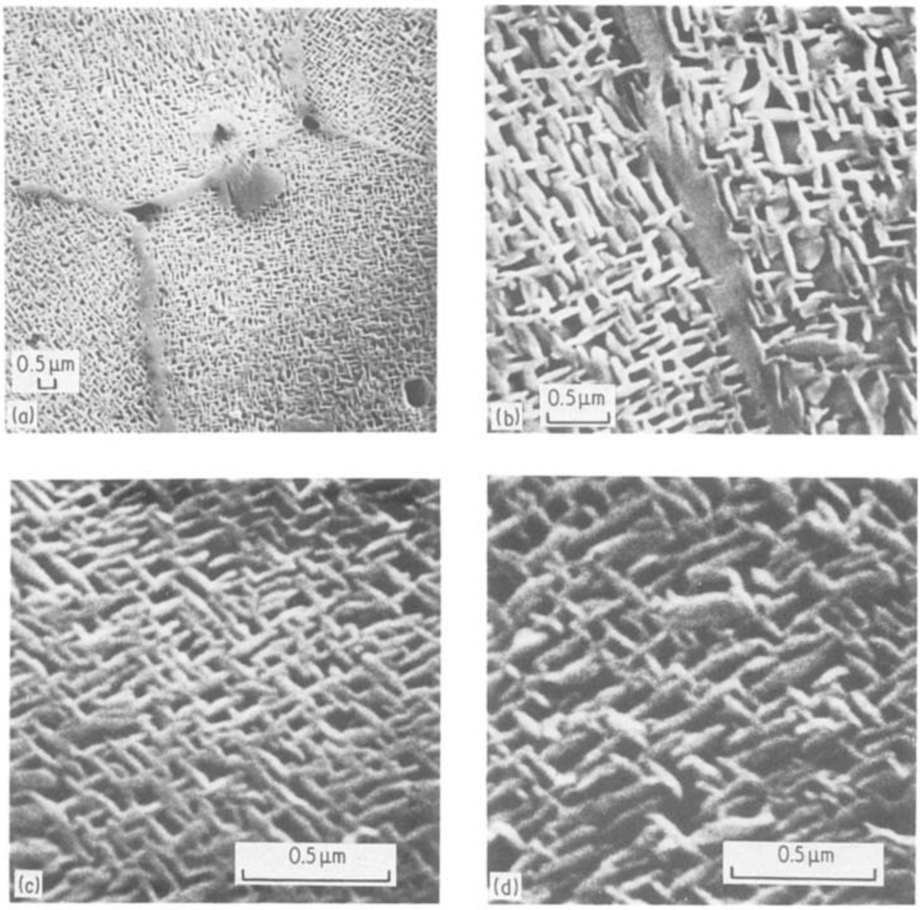

Figure 2 Size of precipitates within cubic ZrO_2 matrix grains of PSZ ceramics. Precipitate structure revealed by etching away cubic matrix with 20% HF solution. (a, b) Sample Ag-1 given longer ageing treatment at 1400° C for 8 h after sintering shows increase in precipitation size compared with (c, d) Samples MS-83 and TS-83 sintered and given normal heat treatment (~ 1450° C for 1 to 2 h).

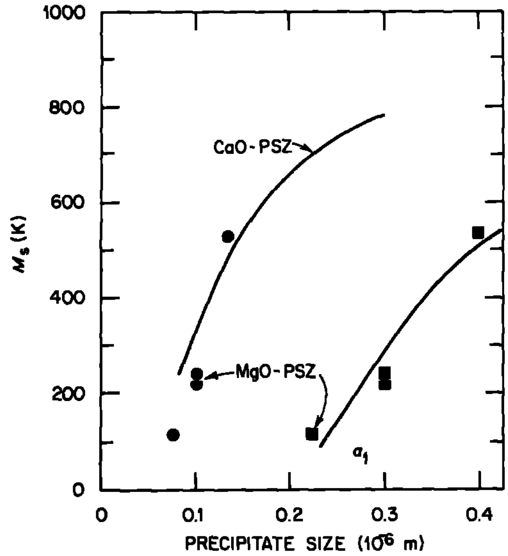

Figure 3 Temperature at which tetragonal to monoclinic transformation (M_s) is initiated during cooling increases with increasing precipitate size. (●) Largest dimension (a_1) of ellipsoidal precipitates in MgO–PSZ suggests a shift in M_s–size behaviour as compared to that in CaO–PSZ containing cuboid precipitates [15]. (■) Mean dimension for precipitates in MgO–PSZ results in behaviour comparable to that in CaO–PSZ.

of particle edges and corners discussed by Rühle and Kriven [16]. However as discussed previously [17, 18], the segregation of magnesium can generate matrix strains due to the formation of δ-$Mg_2Zr_5O_{12}$ during ageing at 1100° C. They observed that this process also triggered the transformation of tetragonal precipitates when the samples were cooled to room temperature. Thus in those PSZ ceramics where the precipitate sizes are quite comparable, it is felt that the introduction of the strains associated with the development of the δ phase in the matrix is responsible for the observed differences in the M_s temperatures.

Examination of the MgO–ZrO_2 equilibrium phase diagram (Grain [19]) indicates that the differences in MgO contents will result in an increase in the tetragonal/monoclinic compared with the cubic content, with a decrease in MgO content. This phase diagram does not indicate any effect of MgO content on the transformation of tetragonal to monoclinic symmetry as is revealed in the Y_2O_3–ZrO_2 phase diagram [20]. In the latter case, the tetragonal phase stability increases with an increase in Y_2O_3 content (i.e. the M_s temperature decreases). The absence of observations of a similar behaviour in the MgO–ZrO_2 phase diagram may be a result of the more limited solubility of MgO ($\ll$ 1 mol %) in the tetragonal ZrO_2 as compared to that of Y_2O_3 (2.5 mol %) at room temperature. However, there is no evidence that an increase in MgO content in the tetragonal ZrO_2 lowers the M_s temperature. Thus in the present MgO–PsZ ceramics it appears that changes in precipitate size are primarily responsible for the changes in M_s temperatures.

Determination of the critical fracture toughness values for the various PSZ ceramics at room temperature reveals a dependence upon the M_s temperature for each material (Fig. 4). It is observed for the case where $T > M_s$ that the K_{IC} value at 22° C increases as the M_s temperature is raised to approach the test temperature. This is consistent with the behaviour predicted by Equation 7 and the contribution of the transformation to the overall toughness of the material, K_{IC}:

$$K_{IC} = K_{IC}^{M} + \Delta K_{IC}^{T} \qquad (8)$$

where K_{IC}^{M} is the toughness of the matrix.

In order to test the validity of Equation 7, the ΔK_{IC}^{T} values were obtained using Equation 8 and a K_{IC}^{M} value of 3 MPa m$^{1/2}$; a plot of the natural logarithms of ΔK_{IC}^{T} and $(T - M_s)$ data should exhibit a slope of -1. The plot of ΔK_{IC}^{T} against $(T - M_s)$ for

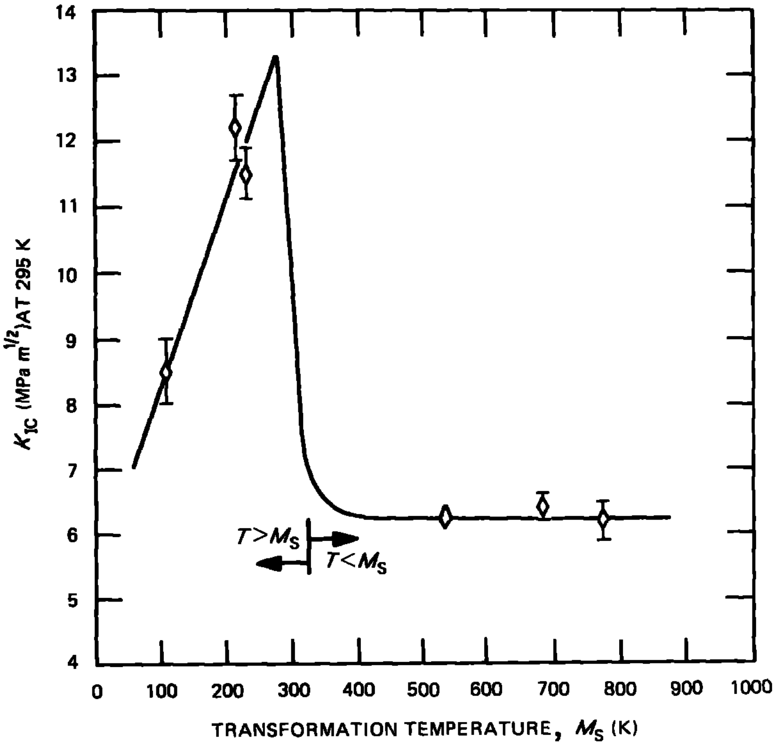

Figure 4 The critical fracture toughness at 22° C (295 K) of the MgO–PSZ ceramics is a function of the M_s temperature of each material. For those PSZ ceramics with $M_s < 22°$ C, the contribution from transformation toughening decreases with decreasing M_s value. When $M_s > 22°$ C, only monoclinic precipitates are present and crack deflection/microcracking processes, rather than transformation toughening, contribute to toughness.

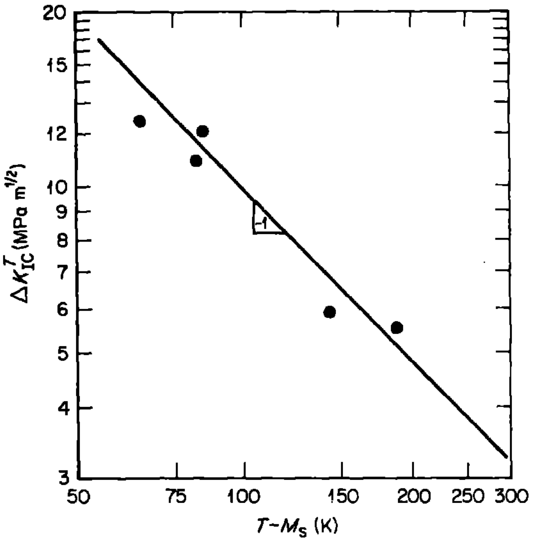

Figure 5 The transformation toughening contribution, ΔK^T_{IC}, increases as $(T - M_s)$ decreases. As predicted from Equation 7, ΔK^T_{IC} is inversely proportional to $(T - M_s)$ for the case where $T =$ 22° C $> M_s$. Note that ΔK^T_{IC} values have been normalized to constant V_f in order to eliminate V_f variations in test samples.

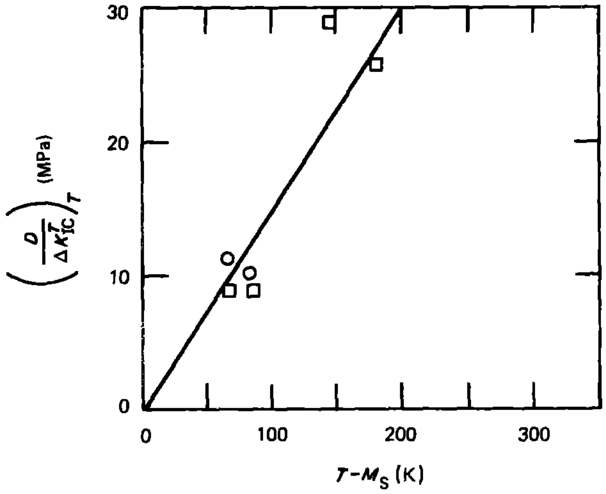

Figure 6 The entropy of the tetragonal to monoclinic transformation at $T =$ 22° C (295 K) can be derived by Equation 9. Fit to experimental data from K_{IC} experiments yields ΔS value of 150 kJ m^{-3} K^{-1} (3.2 J mol^{-1} K^{-1}).

$T =$ 22° C is in excellent agreement with the inverse relationship predicted (Fig. 5).

Confirmation of the behaviour predicted in Equation 7 has at least one practical benefit. One can now use the determination of transformation temperatures (e.g. by thermal expansion, laser Raman or differential thermal analysis), to assess how tough a PSZ ceramic might be. As seen later, the toughness can be estimated. For now it suffices to say that one can see that such bulk measurements allow one to say that materials with M_s temperatures less than but approaching the temperature of interest will be the toughest.

In this case Equation 7 can also be rearranged to

$$D/\Delta K^T_{IC} = (T - M_s)\Delta S \qquad (9)$$

where $D = AB^{1/2}(e^T)^2 V_f E^c K^M_{IC}$ and thus for a given test temperature one can obtain an esimate of ΔS (the reciprocal of the slope) as in Fig. 6. The entropy change will be sensitive to structural/defect changes related to the transformation and hence should be influenced by precipitate size and the amount and type of solute present. Using the MgO–PSZ data, one obtains an entropy value of 150 kJ m^{-3} K^{-1} (3.2 J mol^{-1} K^{-1}) for the stress-induced transformation of the tetragonal precipitates in the cubic matrix. A value of 4.0 J mol^{-1} K^{-1} was obtained for the monoclinic to tetragonal transformation by Coughlin and King [21].

By employing the pertinent data for the current materials, the value of ΔS at 295 K, and Equation 7, we can derive a simplified description of ΔK^T_{IC}. Note that the value of A is 0.4 as determined in additional studies of transformation zone sizes by laser Raman analysis [12]. At 295 K, ΔK^T_{IC} can be estimated by

$$\Delta K^T_{IC} = 2.0 V_f/(295 - M_s) \quad \text{GPa m}^{1/2} \qquad (10)$$

where $M_s <$ 295 K.

One can seen from Equation 9 that ΔK^T_{IC}, and hence K_{IC}, for a given material will be a function of the test temperature for the case where $T > M_s$. Such behaviour is, in fact, observed in the PSZ ceramics (Fig. 7).

If we next consider the toughness data in Fig. 7 in terms of a $(T - M_s)$ funtion where M_s is constant, we can derive a value ΔS as a function of T (Fig. 8). As seen in Fig. 8, the slopes of $D/\Delta K^T_{IC}$ against $(T - M_s)$, based on Equation 9 and the data in Fig. 7, yield two curves which exhibit linear behaviour at lower temperatures and then rise rapidly at higher temperatures. The rapid rise in the *effective* ΔS at higher temperatures simply reflects the fact that the tetragonal phase is very stable and is difficult to transform. This is not a quantitative measure of the entropy change at elevated temperatures. The linear regions indicate that the value ΔS increases with increase in temperature, as expected.

Inspection of Equations 3 and 5 indicates that the critical transformation stress for the MgO–PSZ ceramics can be obtained using either the above thermodynamic data or the zone size data. The critical transformation stress, based on Equation 3 and the above entropy change (Fig. 6) for these ceramics at 22° C is plotted as a function of the M_s temperature in Fig. 9. The results of Becher and Begun [12] using Equation 5 and the zone size data give comparable critical transformation stress levels. The low critical transformation stress levels for some of these materials is reflected in the non-linear stress–strain behaviour which has been observed in some PSZ ceramics [22]. These materials are essentially yielding and plastically deforming like a metal, not by slip but by the phase transformation.

From Fig. 7, we see for the case of $T < M_s$ that the toughness decays over a range of decreasing test temperature which reflects the fact that all the tetragonal phase is not converted to the monoclinic phase until $T = M_f$. At $T < M_f$, the toughness should reach a constant value. In the case of PSZ, this K_{IC} value is 6 to 6.5 MPa m$^{1/2}$ for $T < M_f$. This toughness level is much greater than that of the cubic ZrO$_2$ and is related

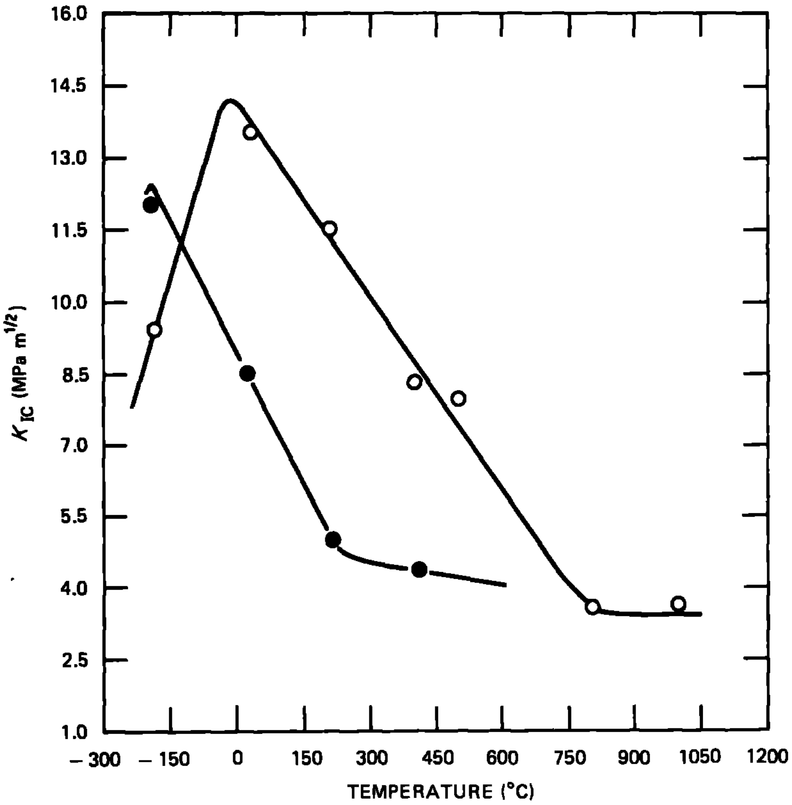

Figure 7 From the thermodynamic considerations of transformation toughening, the critical fracture toughness will be a function of test temperature, T. Plots are for (●) $M_s = 113$ K, (○) $M_s = 218$ K. Experimental results show that when $T > M_s$, K_{IC} decreases with increasing T, i.e. increasing $(T - M_s)$ for PSZ with given M_s. This results from increase in tetragonal phase stability (increase in σ_c^T) as T is raised. When $T < M_s$, a portion of the tetragonal ZrO_2 has spontaneously transformed prior to testing; hence V_f decreases and K_{IC} is lowered. Raising the M_s temperature shifts the peak in K_{IC} to higher test temperatures.

to the compressive matrix strain associated with the transformed monoclinic precipitates, and deflection and branching of the crack by the monoclinic precipitates. Thus the toughness of the PSZ will decay from a peak value at T equal to or, more likely, slightly greater than M_s to a value of $\simeq 6$ MPa m$^{1/2}$ when $T < M_f$ as T is decreased.

The temperature dependence of the transformation toughening results in a range of temperature over which one obtains reasonably high toughness values (i.e. > 6 MPa m$^{1/2}$). From Fig. 7 we can see that this temperature extends from < -190° C to 600° C for the TS-83 and MS-83 PSZ ceramics. It is also apparent that heat-treating the PSZ to introduce multiple populations of precipitate sizes which then have increasing M_s (etc.) temperatures might be used to extend the temperature range of useful transformation toughening, although the peak value of K_{IC} will be lowered. This is a result of the dependence of K_{IC} on the volume fraction of transformable tetragonal precipitates at the temperature of interest which, of course, will be decreased when multiple populations of precipitates are introduced.

It should also be noted that the multiple M_s temperatures exhibited by the TS-83 PSZ can be a result of the introduction of the δ-$Mg_2Zr_5O_{12}$ phase in the

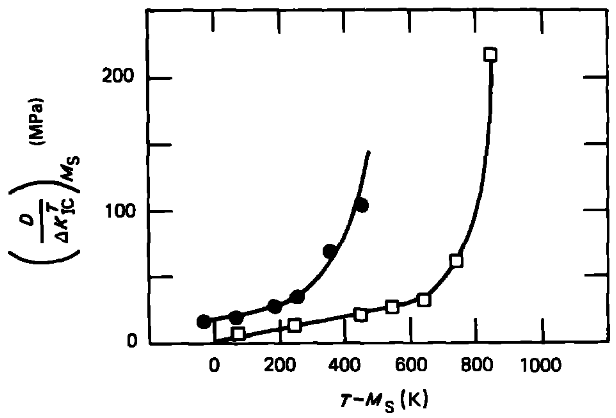

Figure 8 The entropy of the tetragonal to monoclinic transformation will increase with temperature. Using Equation 9 and the data in Fig. 7, one observes that the linear increase in the slope of each curve, ΔS, is constant with initial increase in T where M_s is fixed. Plots are for (●) $M_s = 113$ K, (□) $M_s = 218$ K. At higher temperatures the slopes increase rapidly. While the curves probably do not reflect an absolute value of the increase in ΔS at elevated temperatures, they do indicate that ΔS is increasing with T as one expects.

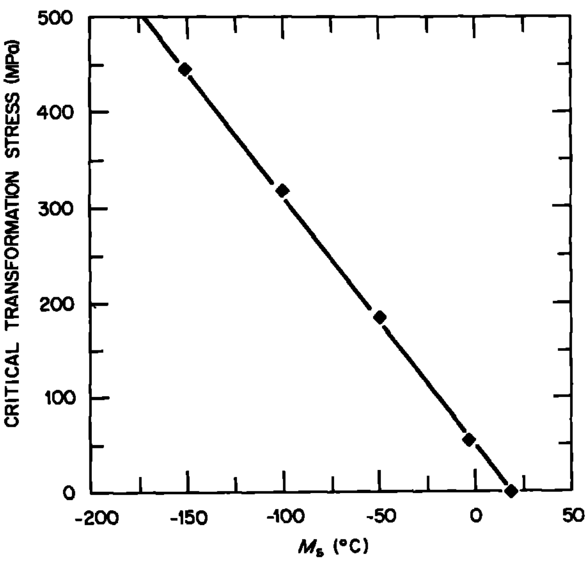

Figure 9 Using Equation 3 and the entropy data in Fig. 6, one can calculate the critical transformation stress. Plot shows the predicted decrease in σ_c^T at 22° C with increase in $M_s \leqslant 22$° C. Note that the σ_c^T range for the MgO–PSZ ceramics studied here is consistent with the observations of Swain [22].

cubic matrix, which results in local matrix strain that makes adjacent tetragonal precipitates less stable. This would raise their M_s temperature to near 1100° C as pointed out by Hannink and Swain [17, 18] and would have an effect on the temperature range of optimum toughness similar to the introduction of multiple precipitate sizes mentioned above.

As observed by Becher, Ferber and co-workers [23, 24], holding the TS-82 PSZ ceramic at temperatures of 800 and 1000° C under stress can result in increasing the M_s temperature with increasing hold time. The kinetics of this process are much slower at 800° C than at 1000° C. The process also results in generation of eutectoid decomposition products of the cubic phase at the matrix grain boundaries with long hold times, which must be controlled to avoid extensive degradation of the PSZ. For example the TS-83 PSZ ceramics held at 1000° C for 336 h at a flexure stress of 60% of its fracture strength at 1000° C contained 80% monoclinic phase and had a toughness of 6.2 MPa m$^{1/2}$ at 22° C. Hannink and Swain [17] showed that heat treating for 2 to 5 h at 1100° C with no applied stress resulted in a peak in room-temperature toughness. Thus one could tailor the ageing process.

This also implies that changes in the toughness with both time at the test temperature and the stress level imposed on the PSZ must be considered in any applications. In the work of Becher and Ferber [23] it was observed that the properties of the TS-83 PSZ did not change after a 1000 h exposure at 500° C with an applied stress of 60% of the fast-fracture stress. Thus for this PSZ ceramic the useful temperature range for both optimum toughness and long-term stability at temperature of the toughness are comparable (i.e. $\geqslant 500°$ C). These features will have to be determined for each PSZ material to ensure reliability.

4. Summary

The fracture toughness associated with the stress-induced transformation of tetragonal ZrO_2 to the monoclinic phase can be described in terms of both the characteristic transformation temperatures, M_s, and the test temperature. When $T = M_s$, the energy required to initiate the transformation is zero and the transformation occurs spontaneously. However, when $T > M_s$, additional energy must be supplied to initiate the transformation. In this case, energy can be supplied by externally applied strain energy, ΔU_{se}, via an applied tensile stress acting on a crack tip.

The value of ΔU_{se} required to achieve transformation toughening can be shown to equal the total energy of the transformation, ΔG_T^{t-m}, which has a positive value as the tetragonal phase is more stable for $T > M_s$. When $T = M_s$, $\Delta G_T^{t-m} = 0$ as ΔG_T^{t-m} is equal to $(T - M_s)\Delta S$ where ΔS is the entropy of the transformation. Using the toughness data obtained for MgO–PSZ, ΔS is found to be 3.2 J mol^{-1} K^{-1} at 295 K and to increase with increasing test temperature.

One can also then derive the transformation toughening contribution for MgO–PSZ by considering the M_s temperature, for $T > M_s$, based on the data obtained in the present study. In the case where $T = 295$ K, ΔK_{IC}^T is given by

$$\Delta K_{IC}^T = 2V_f/(295 - M_s) \qquad \text{GPa m}^{1/2} \qquad (10)$$

so that when M_s approaches T (or vice versa) ΔK_{IC}^T reaches a maximum. In the present materials a value of 12 MPa m$^{1/2}$ could be obtained for ΔK_{IC}^T at 295 K with an M_s value of 218 K. Thus determinations of transformation temperatures can be utilized to estimate the toughness at $T > M_s$ for ceramics employing the transformation of tetragonal ZrO_2 for additional toughening.

Examination of the current PSZ ceramics using SEM studies of polished surfaces that were etched with 20% HF reveals that the M_s temperature is a function of tetragonal ZrO_2 precipitate size. It was observed that M_s increases rapidly with increase in precipitate sizes of 0.2 to up to 0.4 μm. This is similar to the behaviour observed in CaO–PSZ [15]. Note that precipitate size is a major influence on M_s values in the MgO–PSZ system; an additional factor is the development of the loss of coherency and strain associated with the presence/formation of the δ-phase [13, 17, 18, 23]. In the case of Y_2O_3 and similar solutes, solute content is also a significant factor.

The same relationships employed, (e.g. Equation 10) show that the transformation toughening contribution will decrease with increase in the test temperature, T, when $T > M_s$. This is consistent with the behaviour observed in the MgO–PSZ ceramics in the present study. When $M_f < T < M_s$, the toughness decreases as less tetragonal phase is available to transform as T approaches M_f. At $T < M_f$, the toughness reaches a constant value which is $\simeq 6$ MPa m$^{1/2}$ for the current materials.

Acknowledgement

This research was sponsored by the Division of Materials Sciences, US Department of Energy, under contract DE-AC05-840R21400 with Martin Marietta Energy Systems.

References

1. W. M. KRIVEN, W. L. FRASER and S. W. KENNEDY, *Adv. Ceram.* **3** (1981) 82.
2. A. G. EVANS, N. BURLINGAINE, M. DRORY and W. M. KRIVEN, *Acta Metall.* **29** (1981) 447.
3. A. G. EVANS and A. H. HEUER, *J. Amer. Ceram. Soc.* **63**(5/6) (1980) 241.
4. R. H. J. HANNINK, *J. Mater. Sci.* **13** (1978) 2487.
5. C. A. ANDERSON and T. K. GUPTA, *Adv. Ceram.* **3** (1982) 184.
6. B. BUDIANSKY, J. W. HUTCHINSON and J. C. LAMBROPOULOS, *Int. J. Solid. Struc.* **19** (1983) 337.
7. R. C. BRADT, A. G. EVANS, D. P. H. HASSELMAN and F. F. LANGE (editors), "Fracture Mechanics of Ceramics", Vol. 6 (Plenum Press, New York, 1983) p. 289.
8. S. W. FREIMAN, D. R. MULVILLE and P. W. MAST, *J. Mater. Sci.* **8** (1973) 1527.
9. R. COOK and B. R. LAWN, *Commun. Amer. Ceram. Soc.* **66**(11) (1983) C-200.
10. R. C. GARVIE and P. S. NICHOLSON, *Amer. Ceram. Soc. Bull.* **55**(6) (1972) 303.
11. D. R. CLARKE and F. ADAR, *J. Amer. Ceram. Soc.* **65**(6) (1982) 284.
12. P. F. BECHER, G. M. BEGUN and E. E. FUNKENBUSCH, in "Advances in Ceramics: The Science and Technology of Zirconia" (American Ceramic Society, to be published).

13. R. H. J. HANNINK, *J. Mater. Sci.* **18** (1983) 457.
14. S. C. FARMER, T. E. MITCHELL and A. H. HEUER, *Adv. Ceram.* **12** (1985) 152.
15. R. H. HANNINK, K. A. JOHNSON, R. T. PASCOE and R. C. GARVIE, *ibid.* **3** (1981) 116.
16. M. RÜHLE and W. M. KRIVEN, *Ber. Bunsenges. Phys. Chem.* **87** (1983) 222.
17. R. H. J. HANNINK and M. V. SWAIN, *J. Austral. Ceram. Soc.* **18**(2) (1983) 53.
18. R. CHAIM and D. G. BRANDON, *J. Mater. Sci.* **19** (1984) 2934.
19. C. F. GRAIN, *J. Amer. Ceram. Soc.* **50**(6) (1967) 288.
20. R. RUH, K. S. MAZDIYASNI, P. G. VALENTINE and H. O. BIELSTEIN, *Commun. Amer. Ceram. Soc.* **67**(9) (1984) C-190.
21. J. P. COUGHLIN and E. G. KING, *J. Amer. Chem. Soc.* **72** (1950) 2262.
22. M. V. SWAIN, *Acta Metall.* **33** (1985) 2083.
23. P. F. BECHER and M. K. FERBER, *J. Mater. Sci.*, in press.
24. V. J. TENNERY, M. K. FERBER, P. F. BECHER and S. B. WATERS, in Proceedings of 22nd Contractor's Coordination Meeting, SAE, Warrendale, Pennsylvania, 1985, Vol. P-155, pp. 409–418.

*Received 20 January
and accepted 14 March 1986*